RSC Advances

PAPER

View Article Online
View Journal | View Issue

Cite this: *RSC Adv.*, 2024, **14**, 3473

Facile synthesis of sulphur-doped carbon dots (S-CDs) using a hydrothermal method for the selective sensing of Cr^{6+} and Fe^{3+} ions: application to environmental water sample analysis

Akanksha G. Kolekar,[ab] Samadhan P. Pawar, *[ac] Dattatray B. Gunjal,[a] Omkar S. Nille,[a] Prashant V. Anbhule,[a] Sneha V. Koparde,[ac] Ngoc Quang Nguyen,[e] Daewon Sohn,[e] Govind B. Kolekar,[a] Gavisiddappa S. Gokavi[d] and Vishalkumar R. More*[b]

Received 5th November 2023
Accepted 23rd December 2023

DOI: 10.1039/d3ra07545a

rsc.li/rsc-advances

In this work, we used a one-step hydrothermal method to synthesize blue-emission sulfur-doped carbon dots (S-CDs) using jaggery as a carbon precursor. The synthesized carbon quantum dots showed low toxicity, good water solubility, anti-interference properties, and stable fluorescence. When excited at 310 nm, the S-CDs produced bright emission with a quantum yield of 7.15% at 397 nm. The S-CDs exhibited selective and sensitive quenching responses with limits of detection (LODs) of 4.25 μg mL^{-1} and 3.15 μg mL^{-1} for variable concentrations of Cr^{6+} and Fe^{3+}, respectively, accompanied by a consistent linear relationship between fluorescence intensity and these concentrations. Fluorescence lifetime measurements were used to investigate the fluorescence quenching mechanism, which supports the static type of quenching. Outstanding benefits of the developed S-CD based fluorescence probe include its low cost, excellent sensitivity and selectivity, and ease of use for the detection of Cr^{6+} and Fe^{3+} ions. The developed carbon dot based fluorescent probe was successfully used to detect Cr^{6+} and Fe^{3+} ions in real water samples with an excellent recovery ratio.

Introduction

Pollution of heavy metals is a critical concern owing to its harmful effects on the environment and human beings. Heavy metals such as cobalt, iron, mercury, chromium, and lead have a high chemical toxicity toward biological organisms.[1,2] Among them, iron (Fe^{3+}) and chromium (Cr^{6+}) are the most common metal pollutants detected in environmental water bodies.[3,4] Chromium exists in two oxidation states: Cr^{3+} and Cr^{6+}.[5] Cr^{3+} is an essential nutrient for organisms as it exhibits little toxicity and no harm; however, owing to its high oxidation potential, high levels of Cr^{6+} have mutagenic and carcinogenic effects on the human body.[6,7] The United States Environmental Protection Agency recommends that the concentration of Cr^{6+} in potable water should be lower than 100 μg L^{-1}.[8] Therefore, it is necessary to monitor the concentration of Cr^{6+} in real water samples. Fe^{3+} is one of the heavy metals and a main source of water pollution. Therefore, it causes big problems for human health. In cell functioning and biological metabolism, a trace amount of iron (Fe^{3+}) plays an important role in the human body but an excessive amount can put pressure on the liver and subsequently lead to a series of liver diseases.[9] Additionally, the accumulation of Fe^{3+} ions in the environment will cause a great threat to living organisms.

Several approaches have been developed for the accurate and precise detection of Cr^{6+} and Fe^{3+}, including colorimetry,[10,11] electrochemical methods,[12,13] atomic absorption spectrometry, inductively coupled plasma-mass spectrometry,[14–16] chromatography,[17,18] and organic molecular probes.[19,20] However, most of these methods require special instrumentation, hazardous chemicals, and complicated synthesis as well as exhibit water dispersibility of organic molecular probes, low selectivity, and high detection limits. On the contrary, the fluorescence based detection method has many advantages, such as high selectivity, wide linear dynamic range, small interference, low detection limit, and simple sample pretreatment.[20–22]

Carbon dots (CDs) are environment friendly fluorescent nanomaterials exhibiting low toxicity, good water solubility, and

[a]*Fluorescence Spectroscopy Research Laboratory, Department of Chemistry, Shivaji University, Kolhapur 416004, Maharashtra, India. E-mail: sampawar1987@gmail.com*

[b]*Department of Chemistry, The New College, Kolhapur 416012, Maharashtra, India. E-mail: morevishalkumar@newcollege.ac.in*

[c]*Department of Chemistry, Rajarshi Chhatrapati Shahu College, Kolhapur 416003, Maharashtra, India*

[d]*Department of Chemistry, Shivaji University, Kolhapur 416004, Maharashtra, India*

[e]*Department of Chemistry and Research Institute for Convergence of Basic Science, Department of Chemistry, 222 Wangsimni-ro, Seoul 04763, South Korea*

excellent optical properties compared to traditional quantum dots, which are the best alternative to fluorescent probes in biosensors and biological imaging.[23,24] Various raw materials can be used for CD synthesis; these usually include inorganic materials,[25,26] biological materials,[27–29] and waste materials,[30,31] and CDs are mainly synthesized *via* hydrothermal or microwave treatments. However, there are few reports on the use of cheap, easily available, environment friendly Chinese herbal medicine and monomers or extracts of Chinese herbal medicine as a source material for CD synthesis. Currently, there are many studies on using CDs as sensors for metal ion detection, whose main detection principle is the quenching effect caused by the varying affinity between the surface functional groups of the CD and the target. Sun *et al.* synthesized fluorescent carbon quantum dots with *Fructus lycii* as the raw material.[32] Abundant hydroxyl groups on the surface formed a complex with Fe^{3+} through coordination, exhibiting an internal filtering effect, which could quench the fluorescence of CDs. Wu *et al.* synthesized low-cost and environment-friendly photoluminescence carbon quantum dots with giant knotweed rhizome as the carbon source and utilized the interaction between carboxyl and Hg^{2+} on the surface of CDs to form chelates, which were detected through electron or energy transfer.[33]

In this study, sulphur-doped carbon dots (S-CDs) were synthesized by a one-step hydrothermal method using jaggery as a carbon precursor. The S-CDs have bright emission at 397 nm when excited at 310 nm and have good quantum yield. The sulphur-doped CDs were then used for indirect determination of Cr^{6+} and Fe^{3+} in aqueous solution by fluorescence measurement (Scheme 1). The S-CDs exhibit selective and sensitive quenching responses to Cr^{6+} and Fe^{3+} ions with a reliable linear relationship between fluorescence intensity and Cr^{6+} and Fe^{3+} concentrations. Moreover, the developed S-CDs-based fluorescence probe was successfully applied to real water samples with satisfactory results and showed high potential for selective recognition and accurate estimation of Cr^{6+} and Fe^{3+} in a complex matrix.

Experimental

Chemicals and reagents

A jaggery sample was purchased from a local market in Kolhapur, India. All necessary chemicals of analytical reagent grade were procured from SD Fine-Chem, Mumbai, and used as received. All the solutions for measurements were prepared in double distilled water.

Synthesis of fluorescent S-CDs

Sulphur-doped carbon dots (S-CDs) were synthesized by a single-step hydrothermal method using jaggery as a carbon source. Briefly, an appropriate quantity of jaggery and sulphuric acids (H_2SO_4) was taken in a Teflon-lined autoclave having a 50 mL capacity and heated at 180 °C for 8 hours. After completion of the reaction the autoclave was allowed to cool to room temperature and a dark brown solution was obtained. After that, the resultant solution was centrifuged at 10 000 rpm for 15 minutes and filtered by using a 0.22 μm syringe filter to remove large particles and impurities. The resultant solution was subjected to dialysis (molecular weight cut-off was 1000 Da) for 24 hours at room temperature. The synthesized S-CDs solution has an acidic pH (pH = 3) while after the dialysis treatment the obtained S-CDs had a near-neutral pH (pH = 6.0). Finally, the S-CDs were stored in the refrigerator for further use.

Quantum yield measurements (QY)

Quinine sulfate in 0.1 M H_2SO_4 (QY is 0.54 at 360 nm, $\eta = 1.33$) was used as the standard substance to determine the fluorescence QY of synthetic S-CDs,[34] which was determined according to the following formula:

$$QY(\%) = QY_R\left(\frac{I_s}{I_R}\right)\left(\frac{A_R}{A_S}\right)\left(\frac{\eta_S{}^2}{\eta_R{}^2}\right) \quad (1)$$

The quantum yields of S-CDs and quinine sulfate are expressed by QY and QY_R, respectively. '*I*' represents the integrated fluorescence intensity at the same excitation wavelength. '*A*' is the absorbance measured with a UV-vis spectrophotometer. The symbols η_S and η_R represent the solvent refractive index of S-CDs and quinine sulfate, respectively.

Characterization

The morphology and microstructure of the sample were investigated using a JEOL, JEM-2100 Plus transmission electron microscope (TEM). Fluorescence and ultraviolet-visible (UV-vis)

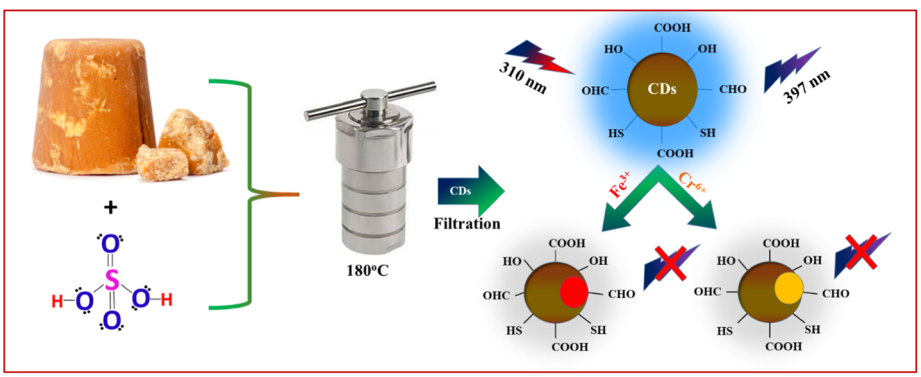

Scheme 1 Schematic representation of the synthesis of S-CDs and their sensing application for the detection Cr^{6+} and Fe^{3+} ions.

absorption studies on the synthesized S-CDs were performed using a JASCO Spectrofluorometer FP-8300 and SPECORD 210 Plus Analytic Jena Spectrometer, respectively. Time-correlated single photon counting (TCSPC) spectrophotometer HORIBA Jobin Yvon IBH employing a nanosecond diode laser (IBH, nano LED-07) was used to measure fluorescence emission decay curves. The crystallinity of S-CDs was characterized using a powder X-ray diffractometer (XRD) (Bruker D8 advance, X-ray diffractometer) with CuKα (λ = 1.5406 Å) radiation with a voltage of 45 kV and current of 40 mÅ. X-ray photoelectron spectroscopy (XPS) was performed to estimate the elemental composition of S-CDs. A Fourier transform infrared (FT-IR) spectroscopic study was performed using a Fourier transform infrared spectrophotometer (Bruker alpha).

Fluorescence behavior of S-CDs at different pH

For the study of fluorescence behavior at different pH values, the as-synthesized S-CDs solution was used. In a typical procedure, the fixed volume of the probe solution and buffers of different pH were diluted to 10 mL and the fluorescence of all the solutions having pH 1 to 11 were obtained at the excitation wavelength 310 nm.

Metal ion detection

The metal ion sensing ability of S-CDs was investigated for different metal ions under identical conditions. One mL of 100 ppm solution of each metal ion and one mL of the synthesized S-CDs solution was diluted to 10 mL and allowed to react for 5 minutes at room temperature. The fluorescence measurements of all these solutions were obtained at an excitation wavelength of 310 nm. To study the Cr^{6+} and Fe^{3+} sensing capacity of S-CDs, different concentrations of Cr^{6+} and Fe^{3+} were diluted to a fixed volume and analyzed similarly.

Real sample analysis

To employ the developed S-CDs-based fluorescent probe for real water analysis, different water samples were collected from the University Campus, Rajaram Lake, and Panchganga River. The collected samples were boiled and filtered to remove the impurities. Filtered samples were spiked with various known concentrations of Cr^{6+} and Fe^{3+} and then mixed with S-CDs solution. The fluorescence study of each sample was recorded after 5 minutes of incubation time at room temperature.

Results and discussion

Characterization of S-CDs

TEM measurements were performed to investigate the morphology and size distribution of the S-CDs (Fig. 1). For the TEM measurement, the sample was prepared by placing the S-CDs solution on a copper grid. The histogram shows that the particle size distribution of S-CDs ranged between 5 nm and 9 nm and the average diameter was 7 nm. The SAED pattern shows circular faded rings, indicating the amorphous nature of S-CDs. The XRD pattern of S-CDs, as shown in Fig. 2, shows a broad peak at $2\theta \approx 26.3°$, which can be assigned to highly disordered carbon supporting the amorphous nature.[35] Additionally, the peak around $2\theta \approx 26.4°$ indicates that there may be doping of sulphur in carbon dots (JCPDS card number 00-001-0478).[36]

Elemental composition and speciation within the S-CDs were determined by XPS. The XPS survey spectrum (Fig. 3) indicates that the S-CDs are mainly composed of carbon, oxygen, and sulphur elements, suggestive of the incorporation of all reagents into the particles. The XPS spectrum show that the prominent peaks around 284 eV and 531 eV are due to carbon and oxygen. Moreover, the peak around 164 eV confirms

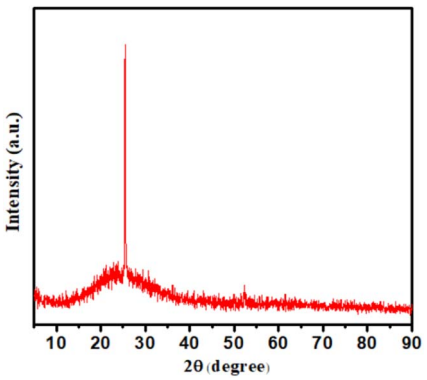

Fig. 2 XRD pattern of the synthesized S-CDs.

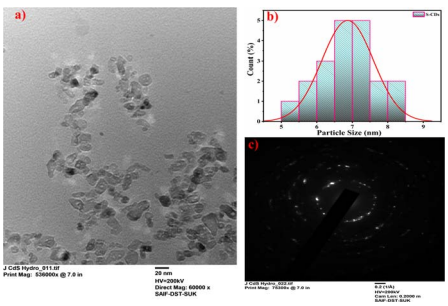

Fig. 1 (a) High resolution TEM image, (b) particle size distribution, and (c) SAED pattern of the synthesized S-CDs.

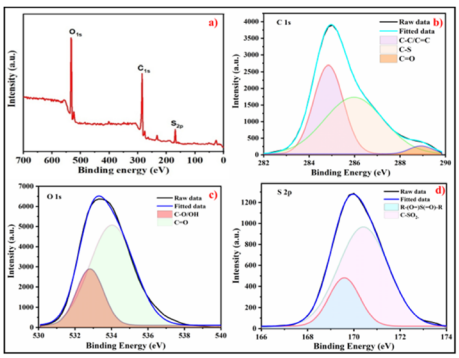

Fig. 3 (a) XPS survey spectrum of the synthesized S-CDs and high-resolution deconvoluted spectra of (b) C 1s, (c) O 1s, and (d) S 2p.

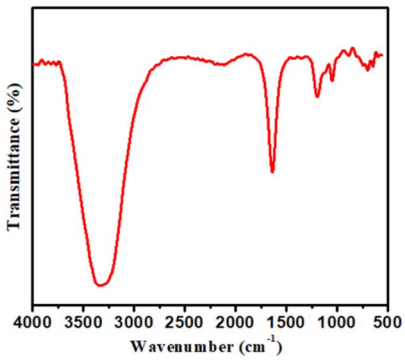

Fig. 4 FT-IR spectrum of the synthesized S-CDs.

the presence of sulphur dopant in the carbon core.[37,38] The high-resolution XPS spectra of C 1s deconvoluted into three peaks correspond to C–C/C=C, C–S, and C=O groups at binding energies of 284.86 eV, 285.97 eV, and 288.94 eV, respectively (Fig. 3b). Fig. 3c depicts the deconvoluted spectra of O 1s containing two peaks at 532.82 eV and 534.03 eV belonging to C–O/O–H and C=O groups, respectively. The S 2p spectra contain two deconvoluted peaks of R–(O=) S(=O)–R and C–SO_{2-} at 169.51 eV and 170.35 eV, respectively (Fig. 3d).[39] The presence of C-, O-, and S-containing surface functionalities makes S-CDs more interactive with metal ions.

The FT-IR spectrum (Fig. 4) showed different characteristic peaks of S-CDs for different functional groups. In the spectrum, a broad peak around 3300 cm^{-1} is of O–H stretching vibrations since S-CDs are well dispersed in water. The peaks at 1680 cm^{-1} are due to C=O. In addition to the carbonyl group, the peak at 1198 cm^{-1} can be assigned to the C–S bond, whereas the peak at 1059 cm^{-1} can be consigned to the C–O bond. FT-IR study concluded that there could be a number of hydrophilic functional groups on the surface of S-CDs, which caused excellent water solubility and helped in complex formation.[35–40]

Optical properties

The optical properties of synthesized S-CDs were studied by UV-vis and fluorescence spectroscopy (Fig. 5). Absorption at 287 nm

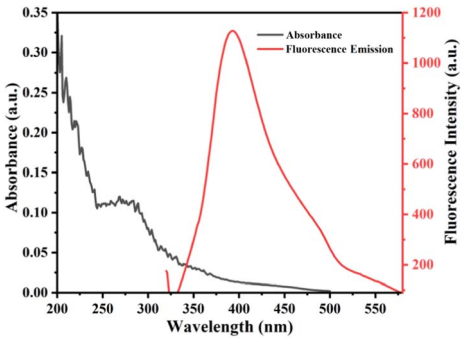

Fig. 5 UV-vis absorption and fluorescence emission spectra of the synthesized S-CDs.

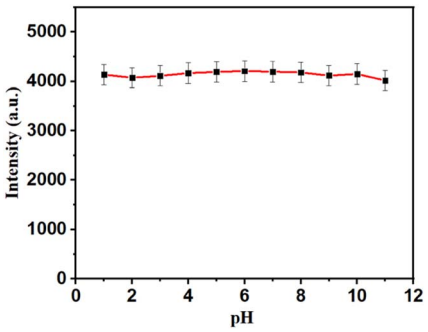

Fig. 6 Effect of pH on the fluorescence intensity of S-CDs.

was observed in UV-vis, which is assigned to $\pi \rightarrow \pi^*$ transition due to the sp^2 domains of C=C from the carbon core. Similarly, emission behavior of S–C-dots at different excitation wavelengths were also studied. The excitation wavelength of 310 nm resulted in maximum emission intensity. Therefore, using an excitation wavelength of 310 nm, the emission behavior of S-CDs was studied at different pH. The result showed that there was not much change in the fluorescence intensity of S-CDs as the pH of the solution increased (Fig. 6). Also, the quantum yield of the as-synthesized S-CDs was determined to be 7.15%.

Effect of pH on fluorescence properties

The effect of pH on the fluorescence properties of S-CDs was investigated at different pH values from 2 to 12. Fig. 6 shows the fluorescence behavior of S-CDs at different pH values. Almost no change in the emission intensity of CDs with pH was observed, which indicated a pH-independent emission nature of S-CDs. The results revealed that the synthesized S-CDs are highly stable with changes in pH.

Selectivity study

To explore the selectivity of the sensor system and the influence of different ions on the fluorescence intensity of S-CDs, each metal ion of 10 μg mL^{-1} was added to the S-CDs solution under optimal experimental conditions. As shown in Fig. 7, S-CDs showed a significant fluorescence reduction in Cr^{6+} and Fe^{3+} in the presence of various metal ions, indicating that S-CDs have good selectivity and a unique effect on Cr^{6+} and Fe^{3+}.

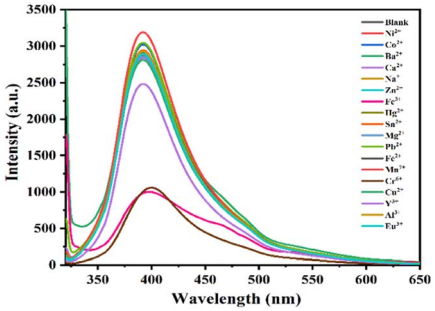

Fig. 7 Fluorescence spectra of S-CDs in the presence of various metal ions.

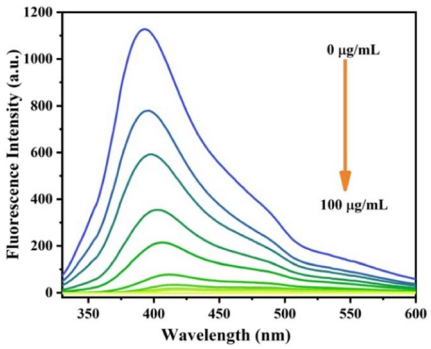

Fig. 8 Fluorescence spectra of S-CDs in the presence of different concentrations of Cr^{6+} (5 μg mL^{-1} to 100 μg mL^{-1}).

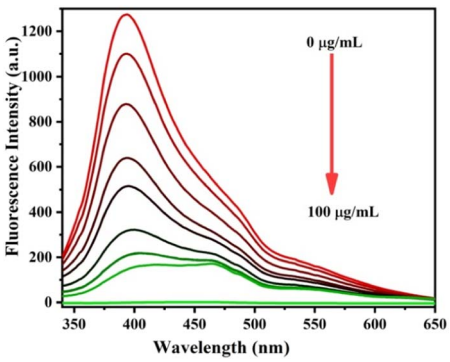

Fig. 9 Fluorescence spectra of S-CDs in the presence of different concentrations of Fe^{3+} (5 μg mL^{-1} to 100 μg mL^{-1}).

To further study the sensitivity of Cr^{6+} and Fe^{3}, the fluorescence spectra of S-CDs after adding different concentrations of Cr^{6+} and Fe^{3+} were recorded^{+}, as shown in Fig. 8 and 9. When the concentration of Cr^{6+} and Fe^{3+} was increased, the fluorescence intensity of S-CDs decreased continuously, confirming the applicability of Cr^{6+} and Fe^{3+} as a "turn-off" fluorescent probe. Fig. 10 and 11 suggest a good linear relationship between Cr^{6+} and Fe^{3+} concentration and the fluorescence intensity of S-CDs in the range of 5 μg mL^{-1} to 30 μg mL^{-1}, and 5 μg mL^{-1} to 70 μg mL^{-1}, respectively. The coefficient of determination (R^2)

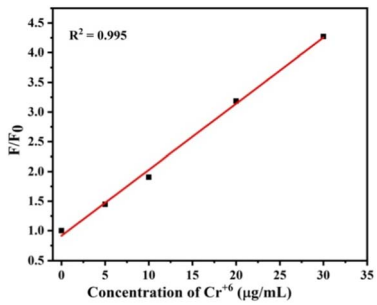

Fig. 10 Linear plots of F/F_0 *versus* the concentration of Cr^{6+} in the range 5 μg mL^{-1} to 30 μg mL^{-1} (F_0 and F represent the fluorescence intensity of the initial and added Cr^{6+}, respectively).

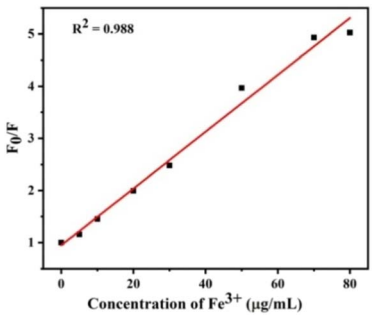

Fig. 11 Linear plots of F/F_0 *versus* the concentration of Fe^{3+} in the range 5 μg mL^{-1} to 70 μg mL^{-1} (F_0 and F represent the fluorescence intensity of the initial and added Fe^{6+}, respectively).

values were 0.995 and 0.988, respectively. The detection limits of Cr^{6+} and Fe^{3+} were 4.25 μg mL^{-1} and 3.15 μg mL^{-1}, respectively, calculated using the formula $3\sigma/k$ (σ is the standard deviation and k is the slope of the calibration curve).

Fig. 10 and 11 suggest a good linear relationship between Cr^{6+} and Fe^{3+} concentrations and the fluorescence intensity of S-CDs in the range of 5 μg mL^{-1} to 30 μg mL^{-1} and 5 μg mL^{-1} to 70 μg mL^{-1}, respectively. The coefficients of determination (R^2) were 0.995 and 0.988, respectively. The detection limits of Cr^{6+} and Fe^{3+} were 4.25 μg mL^{-1} and 3.15 μg mL^{-1}, respectively,

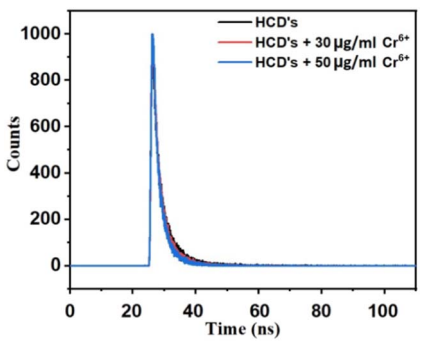

Fig. 12 Plot of the fluorescence decay of S-CDs in the presence of different concentrations of Cr^{6+} ($T_{0\ \mu g\ mL^{-1}} = 2.80$ ns, $T_{30\ \mu g\ mL^{-1}} = 2.40$ ns and $T_{50\ \mu g\ mL^{-1}} = 2.03$ ns).

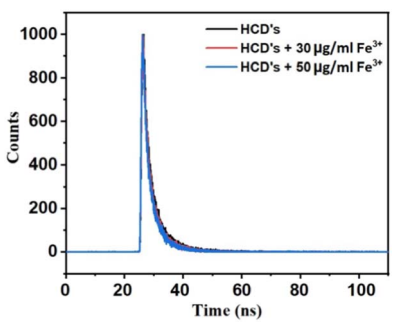

Fig. 13 Plot of the fluorescence decay of S-CDs in the presence of different concentrations of Fe^{3+} ($T_{0\ \mu g\ mL^{-1}} = 2.99$ ns, $T_{30\ \mu g\ mL^{-1}} = 2.94$ ns and $T_{50\ \mu g\ mL^{-1}} = 2.90$ ns).

calculated using the formula $3\sigma/k$ (σ is the standard deviation and k is the slope of the calibration curve).

Mechanism for detecting Cr^{6+} and Fe^{3+} by S-CDs

To explore the fluorescence quenching mechanism of S-CDs by Cr^{6+} and Fe^{3+}, a fluorescence lifetime study was performed. As shown in Fig. 12 and 13, no obvious changes in the lifetime indicated that the fluorescence quenching of CDs by Cr^{6+} and Fe^{3+} is attributed to the static type of quenching effect, *i.e.*, the ground state complex formation takes place between the surface groups of S-CDs and Cr^{6+} and Fe^{3+} ions. The fluorescence quenching of S-CDs by Cr^{6+} and Fe^{3+} could be due to the electrostatic interaction as well as ionic interactions between the negative surface groups of S-CDs and Cr^{6+} and Fe^{3+} ions, which lead to the complexation between them.[35,40]

Cr^{6+} and Fe^{3+} detection in real samples

Standard recovery experiments were performed using tap water, lake water, and river water samples to determine whether the S-CD fluorescence method could be used to determine Cr^{6+} and Fe^{3+} concentrations in real samples, and the results are summarized in Tables 1 and 2, respectively. Each water sample was filtered and then centrifuged at 10 000 rpm for 10 min before analysis. As shown in Tables 1 and 2, the experimental results showed that recoveries of Cr^{6+} and Fe^{3+} reached 97.20–99.25% and 99.87–101.48%, respectively, with the relative standard deviation (RSD) values of 1.17–1.62% and 0.26–0.97%, respectively, all of which were less than 2%.

Table 1 Determination of Cr^{6+} in real water samples

Samples	Spiked ($\mu g\ mL^{-1}$)	Found[a] ($\mu g\ mL^{-1}$)	Recovery (%)	RSD (%) ($n = 3$)
Tap water	5	4.94	98.80	1.17
	10	9.78	97.80	1.21
	20	19.7	98.50	1.30
Lake water	5	4.86	97.20	1.57
	10	9.82	98.20	1.62
	20	19.76	98.80	1.43
River water	5	4.9	98.00	1.33
	10	9.87	98.70	1.26
	20	19.85	99.25	1.35

[a] Mean of three measurements.

Table 2 Determination of Fe^{3+} in real water samples

Samples	Spiked ($\mu g\ mL^{-1}$)	Found[a] ($\mu g\ mL^{-1}$)	Recovery (%)	RSD (%) ($n = 3$)
Tap water	20	20.12	100.60	0.97
	30	29.96	99.87	0.56
	40	40.59	101.48	0.82
Lake water	20	20.29	101.45	0.51
	30	30.1	100.33	0.88
	40	40.33	100.83	0.66
River water	20	20.2	101.00	0.36
	30	30.28	100.93	0.55
	40	40.44	101.10	0.26

[a] Mean of three measurements.

Conclusions

In summary, a simple one-step hydrothermal method for the synthesis of carbon quantum dots, with jaggery as the precursor, showing blue fluorescence emission was established. The Cr^{6+} and Fe^{3+} ion quenches the fluorescence intensity of S-CDs due to electrostatic interaction between negatively charged surface groups of S-CDs and positive ions and it was supported by fluorescence life time study. Therefore, fluorescence analysis platform for the detection of Cr^{6+} and Fe^{3+} was established, which can be used for the sensitive and selective detection of Cr^{6+} and Fe^{3+} in real water samples with limit of detections (LOD) of 4.25 $\mu g\ mL^{-1}$ and 3.15 $\mu g\ mL^{-1}$, respectively, with satisfactory results and broad application prospects in environmentally and biologically related fields.

Author contributions

Conceptualization and methodology: AK, SP, and DG, characterization and data analysis: ON, PA, and SK, writing of the original draft: AK and SP, review and editing: GK, DS, and NN, supervision, conceptualization, writing, reviewing and editing: GG and VM.

Conflicts of interest

The authors declare that they have no competing financial interests.

Acknowledgements

The authors thank the Department of Chemistry, Shivaji University, Kolhapur, the Department of Chemistry, and The New College, Kolhapur for the laboratory facilities and characterizations. Daewon Sohn and Ngoc Quang Nguyene thanks to the National Research Foundation of Korea (NRF) 2020R1A6A1A06046728, 2022R1A2C1010580 and 2022R1A6C101A779-23.

Notes and references

1 Y. Liu, Q. Xue, C. Chang, R. Wang, Z. Liu and L. He, *Anal. Sci.*, 2022, **38**, 55–70.
2 F. Yarur, J. R. Macairan and R. Naccache, *Environ. Sci.: Nano*, 2019, **6**, 1121–1130.
3 H. Zhang, Y. Huang, Z. Hu, C. Tong, Z. Zhang and S. Hu, *Microchim. Acta*, 2017, **184**, 1547–1553.
4 Y. Li, J. Chen, Y. Wang, H. Li, J. Yin, M. Li and L. Chen, *Appl. Surf. Sci.*, 2021, **538**, 148151.
5 S. Zhang, L. Jin, J. Liu, Q. Wang and L. Jiao, *Mater. Chem. Phys.*, 2020, **248**, 122912.
6 N. N. Nghia, B. T. Huy and Y. I. Lee, *Microchim. Acta*, 2019, **186**, 1–7.

7 Y. Shen, Y. Wei, C. Zhu and D. M. Han, *Coord. Chem. Rev.*, 2022, **458**, 214442.
8 F. Ming, J. Hou, C. Hou and Q. He, *Spectrochim. Acta, Part A*, 2019, **222**, 117165.
9 L. Gu, J. Zhang and C. Kong, *Food Chem.*, 2022, **376**, 131898.
10 J. F. Guo, D. Q. Huo, M. Yang and P. Yang, *Talanta*, 2016, **161**, 819–825.
11 S. Balasubramanian, A. Udayabhanu, P. S. Kumar, P. Muthamilselvi, C. Eswari, A. Vasantavada, S. Kanetkar and A. Kapoor, *Int. J. Environ. Anal. Chem.*, 2023, **103**, 2480–2497.
12 L. E. Korshoj, A. J. Zaitouna and R. Y. Lai, *Anal. Chem.*, 2015, **87**, 2560–2564.
13 M. Nosuhi and A. Nezamzadeh-Ejhieh, *Electrochim. Acta*, 2017, **223**, 47–62.
14 E. Yilmaz and M. Soylak, *Talanta*, 2016, **160**, 680–685.
15 Z. Li, Y. Zhang, R. Wang and D. Jiang, *J. Appl. Spectrosc.*, 2022, **89**, 371–380.
16 H. Hagendorfer and W. Goessler, *Talanta*, 2008, **76**, 656–661.
17 F. Roig-Navarro, Y. Martinez-Bravo, F. J. Lopez and F. Hernandez, *J. Chromatogr. A*, 2001, **912**, 319–327.
18 L. Maknun, K. Kińska, I. González-Álvarez and R. Lobinski, *Anal. Chem.*, 2023, **95**, 9182–9190.
19 A. Jebnouni, K. Baatout and M. Majdoub, *Opt. Mater.*, 2022, **134**, 113091.
20 T. Liu, Q. Huang, W. Wu, T. Ren and J. Zhang, *Opt. Mater.*, 2022, **130**, 112568.
21 Y. Zhang, X. Fang, H. Zhao and Z. Li, *Talanta*, 2018, **181**, 318–325.
22 S. Huang, H. Qiu, F. Zhu and Q. Xiao, *Microchim. Acta*, 2015, **182**, 1723–1731.
23 S. Feng, Z. Gao, H. Liu, J. Huang, X. Li and Y. Yang, *Spectrochim. Acta, Part A*, 2019, **212**, 286–292.
24 Y. Liu, W. Duan, W. Song and H. Chen, *ACS Appl. Mater. Interfaces*, 2017, **9**, 12663–12672.
25 L. Li, L. Shi, J. Jia, D. Chang, C. Dong and S. Shuang, *Analyst*, 2020, **145**, 5450–5457.
26 M. Zheng, Y. Li, S. Liu, W. Wang, Z. Xie and X. Jing, *ACS Appl. Mater. Interfaces*, 2016, **8**, 23533–23541.
27 M. Cao, C. Xia, J. Xia, D. Jiang, C. Yu and H. Li, *J. Lumin.*, 2019, **206**, 97–104.
28 Y. Zhang, Z. Gao, X. Yang, J. Chang, Z. Liu and K. Jiang, *RSC Adv.*, 2019, **9**, 940–949.
29 R. Atchudan, T. Edison, S. Perumal, R. Vinodh and Y. R. Lee, *J. Mol. Liq.*, 2019, **296**, 111817.
30 Y. Yu, C. Li, C. Chen, H. Huang, C. Liang, Y. Lou and S. Feng, *Talanta*, 2019, **195**, 117–126.
31 J. Ahn, Y. Song, J. E. Kwon, S. H. Lee, K. S. Park, S. Kim and H. Kim, *Mater. Sci. Eng., C*, 2019, **102**, 106–112.
32 X. Sun, J. He, S. Yang, M. Zheng, Y. Wang, S. Ma and H. Zheng, *J. Photochem. Photobiol., B*, 2017, **175**, 219–225.
33 D. Wu, X. Huang, X. Deng, K. Wang and Q. Liu, *Anal. Methods*, 2013, **5**, 3023–3027.
34 M. Azizi, H. Valizadeh, M. Shahgolzari, M. Talebi, E. Baybordi, M. R. Dadpour and M. Mehrmohammadi, *ACS Omega*, 2020, **5**, 24628–24638.
35 D. B. Gunjal, Y. M. Gurav, A. H. Gore and G. B. Kolekar, *Opt. Mater.*, 2019, **98**, 109448.
36 V. M. Naik, D. B. Gunjal, A. H. Gore and G. B. Kolekar, *Diamond Relat. Mater.*, 2018, **88**, 262–268.
37 H. Ding, Y. Ji, J. Wei, Q. Y. Gao, Z. Y. Zhou and H. M. Xiong, *J. Mater. Chem. B*, 2017, **5**, 5272–5277.
38 Z. Hu, X. Y. Jiao and L. Xu, *Microchem. J.*, 2020, **154**, 104588.
39 X. Chen and J. Che, *Food Chem. Adv.*, 2022, **1**, 100112.
40 W. L. Ang, N. S. Sambudi, A. Mohammad and W. A. Benamor, *Sci. Rep.*, 2020, **10**, 21119.